EUROPEAN FUSION DEVELOPMENT AGREEMENT

EFDA–JET–CP(04)07/03

H. L. Berk, B. N. Breizman, L. Chen, D. E. Eremin, G. Fu, N. Gorelenkov,
M. Gryaznevich, S. Hu, M. S. Pekker, S. D. Pinches, S. E. Sharapov
and JET EFDA Contributors

Theoretical Studies of Alfvén Wave–Energetic Particle Interactions

Theoretical Studies of Alfvén Wave–Energetic Particle Interactions

H. L. Berk,[1] B. N. Breizman,[1] L. Chen,[2] D. E. Eremin,1 G. Fu,[3] N. Gorelenkov,[3]
M. Gryaznevich,[5] S. Hu,[2] M. S. Pekker,[1] S. D. Pinches,[4] S. E. Sharapov[4]
and JET EFDA Contributors*

[1]Institute for Fusion Studies, University of Texas at Austin, Austin, Texas, USA
[2]Department of Physics and Astronomy, University of California, Irvine, USA
[3]Princeton Plasma Physics Laboratory, Princeton, USA
[4]Max-Planck Institut für Plasmaphysik, Garching, Germany
[5]Euratom/UKAEA Fusion Association, Culham Science Centre, Abingdon, UK
** See annex of J. Pamela et al, "Overview of JET Results ",*
(Proc. 20th IAEA Fusion Energy Conference, Vilamoura, Portugal (2004).

Preprint of Paper to be submitted for publication in Proceedings of the
20th IAEA Conference,
(Vilamoura, Portugal 1-6 November 2004)

ABSTRACT

Several topics in the study of Alfvén waves and their interaction with energetic particles are reported. (1) In the second stability regime a new Alfvénic mode (α-TAE) has been found that exists even in the continuum with negligible intrinsic damping and its destabilization by energetic particles is discussed. (2) The alteration of the continuum due to pressure compressibility is found to set a lower frequency limit on the Cascade modes at the value $\sqrt{2}C_S/R$. (CS is the sound speed). (3) Neutral beams planned for ITER is found to contribute to a linear instability drive that is nearly equal to the alpha particle drive and the inferred current generated may allow spatially extended TAE eigenmodes to be excited. A quasilinear model is used to estimate alpha particle losses. (4) The rate of frequency sweeping of TAE modes excited on MAST has been used to estimate internal fields leading to results that are compatible with Mirnov coil mearsurements. (5) A numerical model, developed to attempt to understand damping due to kinetic Alfvén excitations of TAE modes, did not produce KAW's in the plasma center and the dominant damping mechanism came from the continuum resonance arising from the decrease of density at the plasma edge.

INTRODUCTION

The self-consistent response of energetic particles in fusion plasmas is a very important area to understand when burning plasma conditions are achieved especially under advanced tokamak (AT) operation. In this presentation we review some recent progress made on the study of the self-consistent interaction of energetic particles with Alfvén waves which includes conditions of interest in AT operation. In section 1 we discuss instability caused by energetic particles on a new Alfvén wave (α-TAE) that can be generated in second stability operation. In section 2 we report on the modification of the lower frequency range of the Cascade mode that is readily triggered in reversed shear operation at finite β. In section 3 we discuss the effect of MeV beams, which are planned to be used for current drive in ITER, on the TAE instability in a burning plasma. In this section a brief description is also given of expected broadening of alpha particles due to their quasi-linear relaxation to TAE excitation. In section 4 we discuss how internal fields have been inferred on MAST by observing fast frequency sweeping of TAE modes. In section 5 we discuss a relatively simple numerical model that attempts to understand the source of damping due to mode conversion that has been reported in several large numerical codes.

1. NEW TOROIDAL ALFVEN MODES

Alfvènic instabilities have been investigated in the high- β second ballooning stable regime using a gyrokinetic-MHD hybrid simulation code. Here, b is the ratio between plasma and magnetic pressures. The physical model is formulated for a two-component (core and energetic) plasma employing the high-*n* ballooning-mode representation and the (*s,* a) model equilibrium where *s* is the magnetic shear and a the standard plasma pressure gradient parameter. The core component is treated as an ideal MHD fluid, which supports the Alfvén eigenmode while the energetic component provides the kinetic instability drive. We find a new type of discrete Alfvén -ballooning eigenmode,

the α-TAE, which is destabilized by energetic particles via wave-particle resonances. This mode is trapped inside the α-induced potential wells and it experiences negligible continuum damping even at frequencies far from the toroidal Alfvén frequency gap [1]. The mode exists even without energetic particles as distinguished the modes from the EPM (energetic-particle modes). Instability is driven by the typical resonance of a wave with the precessional and/or bounce frequencies of the energetic particles. For an axisymmetric toroidal plasma with a large aspect ratio (i.e., $\varepsilon = a/R \ll 1$) and shifted circular magnetic surfaces, the Alfvén -ballooning instabilities are governed by the generalized vorticity equation [2,3],

$$\frac{(1 + 2\varepsilon_0 \cos\theta)}{\omega^2_{A0}} \frac{\partial^2 \delta\psi}{\partial t^2} = \frac{\partial^2 \delta\psi}{\partial \theta^2} - (V + V\rho)\, \delta\psi - \frac{q^2 R^2}{f^{1/2}} \frac{4\pi q_E}{c^2} \langle \Omega_d J_0 \delta G \rangle,$$

where $\omega_A = V_A /(qR)$, VA is the Alfvén speed, $\varepsilon_0 = 2(_e + d\Delta/dr)$, D is the Shafranov shift, q is the safety factor, q_E and m_E are, respectively, the charge and mass of energetic particles, $\omega_d = \omega_k + \omega_p = k_\Theta \Omega_d \omega_k$, wk and ωp are, respectively, the curvature and gradient drift frequencies of energetic particles, $J_0 = J_0 (\sqrt{f}\, k_\theta v_\perp/\omega_c)$ is the Bessel function, $f = 1 + [s(\theta - \theta_k) - \alpha \sin q]^2$, $\alpha = \alpha_c + \alpha_E$, $V = (s- \alpha \cos \theta)^2/f^2 - \alpha \cos \theta/f$ is the potential due to the ballooning curvature effect, and V_ρ is the finite Larmor radius correction of energetic particles to V; with $-\infty < \theta < \infty$ being the extended poloidal angle coordinate along the magnetic field. Note that in Eq. (1), the left-hand side is the inertial term and the right-hand side consists of the field-line bending (first term), the ballooning drive (second term), and the energetic-particle kinetic compression (third term). The energetic component, described by the function δG, is governed by the gyrokinetic equation [2,3]. The energetic particle dynamics is determined by the bounce and precessional motions, along with the free energy source in both configuration and velocity spaces. The kinetic excitations of α-TAEs are displayed in Fig.1 for various poloidal wavenumbers, denoted by $k_\theta \rho_{A0}$ with $k_\theta = nq/r$, and a = 2.0. The unstable mode structures corresponding to, for example $k_\theta \rho_{A0} = 0.32$ are essentially the same as that of the α-TAE trapped in the potential well as shown in Fig.2. The excitation mechanism is characterized by the bounce-precessional resonance condition $wr - vd - K\, wb = 0$ with K being an integer [2], which maximizes the kinetic drive in Eq. (1). With the Maxwellian distribution function for the trapped energetic particles, it is found that the $K = 2$ resonance dominates the α-TAE excitation shown in Fig.2. The quasi-marginal stability of α-TAE is further demonstrated by essentially thresholdless excitations with respect to the energetic-particle drive. In addition to the lowestorder α-TAE, with frequencies $w_r / w_{A0} \approx 0.4$ trapped in the dominant potential well, a higher-order α-TAE, trapped in the neighboring higher-order well, is destabilized with frequencies $w_r / w_{A0} \approx 0.3$ for $k_q r_{A0} \sim 0.1$ in Fig.1. Due to the lower potential barrier, the higher-order α-TAE experiences a relatively stronger continuum damping via wave energy tunneling and thus requires a small but finite excitation threshold in the energetic-particle drive. Meanwhile, the $K = 1$ bounce-precessional resonances are observed for this lower-frequency α-TAE.

In summary, Alfvén instabilities in the second ballooning stable regime are predicted to be dominated by the kinetic excitations of the trapped discrete α-TAEs, which can experience either negligible or finite but small continuum damping.

2. LOW FREQUENCY RESPONSE OF CASCADE MODE

In shear reversed tokamak discharges containing magnetically trapped energetic particles it is common to see multiple Alfvèn cascade modes [4,5] that rise in frequency to the TAE gap as the minimum value of the safety factor, q_0, decreases in time. Theoretical [6,7] and numerical studies [8,9] have shown that the mode is established in a plasma about the shear reversal point. The theory predicts that at very low values of plasma beta the Alfvèn cascade modes are localized about $q(r)=q_0$ and follow an approximate dispersion relation $\omega=/k_{//}/V_A$ with $k_{//} = (n - m/q_0)/R$ until the TAE frequency, $\omega_{TAE} =V_A/(2q_0R)$, is reached. The theory gives strong preference to modes with rising frequency, corresponding to $k_{//} < 0$, which is consistent with most of the experimental data [4,5] where predominantly rising frequency modes are observed [8,9]. Observations also reveal that the modes never reach zero frequency. The spectral lines either disappear at low frequencies or they approach a common minimum frequency for several modes as shown in Fig.3, a less frequent experimental case where downshifting frequency is observed. At low frequency continuum damping [10] together with other damping mechanisms can readily account for mode suppression but not for spectral line bending seen in Fig.3 at the lowest frequency. The latter requires a different underlying mechanism associated with finite plasma beta and geodesic curvature.

The geodesic curvature from toroidal geometry precludes shear Alfvén perturbations from being strictly incompressible, giving rise to pressure perturbation in a finite β plasma. Significant modification of the Alfvén continuum due to plasma pressure was found numerically in Ref. [11]. This finding is apparently relevant to what is seen in Fig. 3 because it appears that the cascade frequency tends to be close to the continuum, except when the mode reaches the TAE gap. However, Ref. [11] does not immediately give the precise physics reason for the relatively strong pressure effect on low-frequency cascades. This calls for analytical treatment of the problem [12], which enables parametric comparison of the underlying mechanisms and identification of the dominant one.

In addition to the geodesic effect, there are two more pressure effects on shear Alfvén waves, which are convection in presence of an equilibrium pressure gradient and the toroidicity induced coupling between shear Alfvén waves and acoustic modes. Such coupling occurs at $\omega = C_S /Rq_0$, where locally the shear Alfvén frequency matches the acoustic frequency for a neighboring poloidal mode number.

The geodesic effect can be clearly separated from both the convection and the acoustic coupling. In contrast to the convective mechanism, the geodesic effect involves plasma compression, and the resulting characteristic frequency scales as $\beta^{1/2}$ rather than β with plasma pressure, which makes the convective mechanism insignificant at sufficiently low pressure. Ironically, plasma compressibility can be difficult to treat in MHD codes, which recently led to an artificial exclusion of the geodesic effect from the simulations of cascade modes in low-beta plasma in favor of less relevant but more

easily incorporated convective effect [13]. The key distinction between the geodesic compressibility and acoustic coupling is that geodesic compression occurs without plasma displacement along the magnetic field lines, and the corresponding characteristic frequency is $\sqrt{2}\, q_0$ times greater than $\omega = C_S/Rq_0$. As a result, the mode phase velocity is greater than the ion thermal velocity even in isothermal plasma, which allows the mode to avoid strong ion Landau damping.

In deriving the mode equation for frequencies below the TAE gap we use the large aspect ratio, low β, and low shear simplifications. After suitable algebra, the MHD equations in the large-*m* limit

reduce to a form that is diagonal in the poloidal harmonic *m* . Using a normalized radial coordinate $x \equiv m(r-r_0)/r_0$ relative to the radial point, r_0 , of zero shear the governing equation for the eigenmode in the region $-1/2 < m - nq_0 < 1/2$ is found to be,

$$\frac{d}{dx}\left[S + x^2\right]\frac{d}{dx}\Phi_m - \left[S + x^2 - Q\,\frac{\omega q_0 R}{V_A\,(mn - nq_0)}\right]\Phi_m = 0,$$

with the following expressions for the quantities *S* and *Q* in the limit $\delta \equiv 1/(2q_0^2) << 1$:

$$S = \frac{m}{4\,(m - nq_0)}\, q_0 \left(r_0^2\,\frac{d^2 q_0}{dr^2}\right)^{-1}\left[\omega^2\,(2q_0 R/V_A)^2 - 4\,(m - nq_0)^2 - 8q_0^2\, C_s^2/V_A^2\right]$$

$$Q = q_0 \left(r_0^2\,\frac{d^2 q_0}{dr^2}\right)^{-1}\left[-\frac{4\pi e}{cB} V_A \frac{R}{r_0}\frac{d}{dr} < n_{\text{fast ion}} > + \frac{2m\,(m - nq_0)\,(r_0/R + 2\nu)}{1 - 4\,(q_0 n - m)^2}\,\frac{r_0}{R}\right].$$

At *x=0*, the Alfvén continuum frequency, ω_{cont}, corresponds to *S=0,* so that the minimum continuum frequency is $\omega_{min} = \sqrt{2}\, C_S/R$. All low-frequency eigenvalues of the mode equation are close to w*cont*. If $0 < (m-nq_0) < 1/2$, the cascade eigenmode is localized around *x=0*, and its eigenfrequency is somewhat greater than w*cont* as seen in Fig.4 (this figure shows eigenfrequencies for a more general set of equations that remains valid even when the frequency enters the TAE band). It is worth mentioning that Eq.(3.1) does not have suitable solutions in the region $-1/2 < m - nq_0 < 0$ where the mode would exhibit a down sweep. Similar to the upward sweeping spectral lines, the atypical down sweeping lines in Fig.3 follow the time evolution of ω_{cont} but their precise interpretation still remains to be developed.

In applying the theory to the JET experiments we note that q_0 typically varies from 4 to 2 in the shear reversed discharges, so that δ is indeed small in such experiments. In Fig.3 we see that the minimum frequencies are an appreciable fraction of the TAE frequency for quite low beta. The lower limit of the continuum frequency, which is independent of *n* or *m* number, appears to be the main governing factor for determining the minimum frequency in Fig.3.

3. EFFECT OF NEUTRAL BEAM ON TAE'S IN ITER

The injection of 1 MeV neutral beams is being planned for ITER as a source of heating, current drive, profile control and for establishing transport barriers [14]. These neutral beams are super-Alfvénic so that they are destabilizing to TAE modes [15]. Though typically the beam pressure is 0.2-0.5 of the alpha particle pressure, the linear universal instability drive of the beam is comparable to the alpha particle drive because the phase space density at the particle- wave resonance for a given beta is larger for a beam distribution than for an isotropic distribution. In addition the pitch angle anisotropy of the distribution allows for an inverted energy distribution (i.e. $\delta f/\delta E > 0$) to be established. The appropriate distribution function, caused by classical slowing down and pitch angle scattering processes, is generated by the Monte Carlo code in TRANSP. However the intrinsic noise of the code makes it difficult to replicate a smooth distribution function that can be used in the stability codes, such as the NOVA-K code. Consequently simplifying theoretical models were developed based on beam injection peaked about some pitch angle when there is relaxation due to electron and ion drag and pitch angle scattering. Satisfactory replication of the distribution predict by TRANSP was obtained as shown in Fig.5.

Typically global TAE modes are more difficult to self-excite than core localized TAE modes as the global mode is damped by continuum resonances that arise within the inner profile of the plasma. However, with neutral beam off-axis injection, we have found that the q-profile, due to the current induced by the neutral beams, can be fairly flat at $r/a \sim 0.4$, where the energetic particle drive is largest. The relatively small value of shear ($s < 0.3$) that exists there prevents an appreciable component of the TAE mode structure from propagating to smaller radii [16], where continuum damping would arise, but allows a global mode structure to arise outside this radius as is seen in the mode shown in Fig.6. The results of the stability analysis for a nominal ITER case is shown in Fig. 7. We see that by neglecting the beam drive the system would be barely stable for the plasma temperature ~20KeV, but with the inclusion we find that the system is significantly above marginal stability. A detailed break-down of the principal partial growth rates, $\gamma_j/\omega(\%)$, for the n=10 TAE mode give: -0.18 from electron collisions, -0.61 from ion Landau damping, -0.43 from radiation of KAW's, 0.82 from alpha particles, 0.71 from neutral beams. Summing the entire result give $\gamma\text{total}/\omega=0.31$.

A heuristic quasilinear model was developed to attempt to assess the nonlinear consequences of the TAE instability [17]. The model builds upon the 1-dimensional model analyzed in Ref. [18] while incorporating the point that only about a quarter of the energetic particle distribution function has undergone relaxation from the resonant particle interaction [19]. The details of this model can be found in the appendix of Ref. [17]. Typically the instability drive is peaked off-axis and the system is locally stable near the axis (due to ion Landau damping) and near the edge due to large electron collisional damping. Under the assumptions that the stability conditions are spatially local and that the quasilinear theory produces overlap of the particle-wave resonances, it follows from that linearly unstable region will spread out radially. However, for a system not too much above the instability threshold the broadened instability band can still remain inside the plasma. The theory allows us to estimate the relaxed distribution function when the outer boundary of the unstable

region is less the edge radius α. However, if the outer boundary of the edge region reaches the edge, alpha particles are directly lost and we can determine the fraction of alpha particle loss as a function of β_α which increases with ion temperature as shown in fig.8.

4. SPECTRAL DETERMINATION OF INTERNAL FIELDS DUE TO FREQUENCY SWEEPING

Rapid up and down frequency sweeping has been observed in several tokamak experiments e.g. [20,21] where TAE modes have been excited by energetic particles. A particularly clear example of thiseffect has been seen in the MAST data shown in Fig.9. A plausible mechanism to explain such sweeping phenomena is the formation of phase space structures in the form of holes and clumps. A general theory, together with numerical simulation studies, has been developed to describe the evolution of phase space structures [22] for waves near marginal stability where the wave exists in the absence of energetic particles and the marginal point is determined by the balance of the perturbing energetic particle drive and background dissipation. When the collisionality is sufficiently small, a near threshold theory [23] shows that the nonlinear evolution is explosive, which implies that the ultimate saturation level is independent of the closeness to marginal stability. Instead the amplitude of the saturated induced field is dependent on the strength of the energetic particle drive and insensitive to the damping mechanisms. The saturated field amplitude (expressed in terms of the nonlinear trapping frequency of a typical resonant particle $\omega_b \propto \delta B_r^{1/2}$(where δB_r is the perturbed radial magnetic field) is found to be $\omega_b = C_2\, \gamma_L$, while the updown frequency sweeping shifts are found to depend on the internal field, $\delta\omega = C_1\, \omega_b^{3/2}\, \delta t^{1/2}$. For a given physical system the dimensionless parameters C_1 and $C2$ can be extracted by examining the response of simulation codes, such as the HAGIS code [24]. An example of the frequency sweeping observed in this simulation is shown in figure 10 where we see up-down frequency sweeping with the frequency shift fitted to the theoretical evolution. Using the MAST geometry, the MISHKA code was employed to find the appropriate TAE eigenfunction for use in the HAGIS simulations which predicts the evolution of theamplitude and phase. The HAGIS code also enabled the direct extraction of the relationship between the nonlinear particle trapping frequency and the perturbed magnetic field amplitude δB_r . Through this approach [25] it was inferred that the observed MAST frequency sweeping mode has a peak internal field amplitude of $\delta B_r \approx 2 \times 10^{-4} T$, while the experimental Mirnov coil measurements, together with the MISHKA code TAE eigenfunction inferred a peak field amplitude of $\delta B_r \approx 5 \times 10^{-4} T$. This result indicates that the frequency sweeping data gives a reasonable estimate of the internal field. However, the methodology of comparison is still needs refinement and is under development.

5. DAMPING DUE TO KINETIC ALFVEN WAVE

A key issue for predicting Alfvèn instability is the correct determination of background damping mechanisms and it is recognized that conversion to radiating KAW's plays a crucial role. A recent experimental test of a TAE damping model showed that a physical understanding of the damping

mechanism is still lacking [26]. In particular, the measured damping rates of an $n = 1$ TAE mode in JET are much larger than the radiative damping rate of KAW's as calculated locally by the NOVA-K code [27]. On the other hand, global gyrokinetic calculations of the PENN [28] and CASTOR [9] codes yielded damping rates comparable to experimental values for low damping rates, $|\omega / \gamma| \leq 2\%$. In the PENN code the principal damping mechanism is due to mode conversion to a KAW near the center of plasma [28] while the results of CASTOR code showed that the damping comes mainly from edge region [9] due to mode conversion to a KAW there. In this work, we develop a model for a large aspect ratio tokamak and show that, when the density at the edge vanishes, that continuum resonance arises near the edge to produce mode damping rates comparable to the measurement and that no mode conversion to KAW is found near the center of plasma.

We start from coupled reduced kinetic equations for TAEs in a large aspect ratio and low beta tokamak and find:

$$\nabla_\perp^2 g_{Km} \nabla_\perp^2 \Phi_m + L_m \Phi_m = L_{m-1} \Phi_{m-1} + L_{m+1} \Phi_{m+1}$$

$$L_m = \frac{1}{r} \frac{d}{dr} r \left(p\omega^2 - k_{\parallel m}^2\right) \frac{d}{dr} - \left(f - k_{\parallel m}^2\right) \frac{m^2}{r^2} + \left(k_{\parallel m}^2\right) \frac{1}{r},$$

$$L_{m-1} = \frac{1}{r} \frac{d}{dr} r\hat{\varepsilon} \left[p\omega^2 \frac{d}{dr} + 2p\omega^2 \frac{m(m-1)}{r^2} \right.$$

$$L_{m+1} = \frac{1}{r} \frac{d}{dr} r\hat{\varepsilon} \left[p\omega^2 \frac{d}{dr} + 2p\omega^2 \frac{m(m+1)}{r^2} \right.,$$

$$g_{Km} = k_{\parallel m}^2 \left[\frac{3}{8} \rho_i^2 + \frac{3}{8} \rho_s^2 \left(1 - 2x_e^2 - i x_e \exp\left(-x_e^2\right) \right) - i\eta\omega \right]$$

where $\hat{\varepsilon} = 2(r/R + \Delta')$, $x_e = \omega / k_\parallel v_e$, ρ, ρ_i, ρ_s are respectively, the mass density, ion Larmor radius, and $r_s = (Te / Ti)^{1/2} r_i$ and η the plasma resistivity (time c^2 in cgs units). Here the operator L_m corresponds to the ideal MHD equation for shear Alfvèn waves in a cylinder with m being the poloidal mode number, and operator $L_{m\pm1}$ arises from toroidicity. Finally the fourth-order term g_{Km} comes from finite ion gyroradius effects, and the parallel electric field due to kinetic electron response and resistivity η.

Equation (1) is solved as an eigenvalue problem using a cubic finite element method. We- consider parameters and profiles of a JET discharge (#38573) at $t = 5$ sec: $B = 2.56$ T, $n_e(0) \sim n_i(0) = 1.75 \times 10^{13} \mathrm{cm}^{-3}$, $T_e(0) = 2.6$KeV, $T_i(0) = 2.0$KeV, $q(0) = 1.36$, and $q(a) = 4.6$. In Fig. 11 we exhibit the damping rate of the $n = 1$ TAE for two cases: the first with finite edge density $n_i(a) / n_i(0) = 0.07$ and the second with zero edge density. In the first case, the $n = 1$ continuum spectrum gap structure is completely open so discrete TAE modes can exist without wave resonance from the Alfvèn

continuum. In this case, we find that there is no evidence of any mode conversion to KAW near the center of plasma. Only negligible mode conversion occurs near the q = 1.5 gap where the main MHD TAE is located. The resultant radiative damping rate is very small $\gamma_d / \omega < 0.1\%$ (see lower curve in Fig.11) due to small ρ_i and ρ_s, consistent with the local model of radiative damping. Furthermore, at the edge no mode conversion to KAW is found for the boundary condition used (i.e., tangential electric field being zero at the plasma edge with a conducting wall). For some other type of boundary conditions, we can show both analytically and numerically that mode conversion can occur near the edge which results in damping rates comparable to the experimental values. Therefore it remains a possibility that additional damping occurs from a more accurate modeling of the plasma-vacuum interface where additional mode conversion and dissipation may occur.

We now consider damping in the second case where continuum resonance occurs near the edge where $n_i(a)=0$. The calculated damping is shown in upper curve in Fig. 11. We observe that in this case the damping rate is much larger than the damping for the case of finite edge density. The dependence of damping with $q(0)$ is correlated to where the eigenmodes peak relative to the edge, with larger damping for modes nearer the edge. The damping is comparable to the experimental values ($\gamma_d / \omega \approx 1\%$) . This result indicates that edge continuum damping is a plausible mechanism for the damping observed for the n=1 TAE modes in JET.

In conclusion, we find that our modeling does not produce any mode conversion from TAE to KAW's near the center of plasma for the parameters and profiles of a JET plasma. There is also insignificant mode conversion near the edge plasma when there are no continuum resonances there. However, accounting for a low density edge region typically allows continuum damping and may account for the observed damping of n=1 modes in JET plasmas.

ACKNOWLEDGEMENTS.

This work is supported by DOE Grants, DE-FG03-94ER54736, DE-AC02-76CH03073 and NSF Grant ATM-0335279.

REFERENCES

[1]. HU, S., and CHEN, L. Chen, Phys. Plasmas **11**(1) (2004) 1.

[2]. CHEN, L., and HASEGAWA, A., J. Geophys. Res. **96**(A2) (1991) 1503.

[3]. CHEN, L, Phys. Plasmas **1**(5) (1994) 1519.

[4]. KIMURA, H. et al., Nucl. Fusion **38** (1998) 1303.

[5]. SHARAPOV, S. E. et al., Phys. Lett. A **289** (2001) 127.

[6]. BERK, H. L. et al. Phys. Rev. Lett. **87** (2001) 185002.

[7]. BREIZMAN, B. N. et al., Phys. Plasmas **10** (2003) 3649.

[8]. FUKUYAMA, A. et al., Proc. 6th Tech. Commmittee on Energetic Particles in Magnetic Confinement Systems, Naka (IAEA, Vienna, 1999).

[9]. BORBA, D. et al., Nucl. Fusion, **42** (2002) 1029.

[10]. ZONCA, F. et. al., Phys. Plasmas **9**, 4939 (2002).
[11]. CHU, M. S. et al., Phys. Fluids B **4** (1992) 3713.
[12]. BREIZMAN, B.N. and PEKKER,M.S, 2004 US TTF meeting April 29 -May 2, Salt Lake City, Utah
[13]. KRAMER, G. J. et. al. Plasma Phys. Control. Fusion **46**, (2004) L23
[14]. CAMPBELL, D. J., Phys. Plasmas **8** (2001) 2041.
[15]. GORELENKOV, N. N. et al., Nuclear Fusion **43** (2003) 594.
[16]. ROSENBLUTH, M. N. et al., Phys. Fluids **4** (1992) 1806.
[17]. GORELENKOV, N.N. et al., PPPL report #39983998, submitted to Nucl. Fusion.
[18]. BREIZMAN, B. N. et al., Phys. Fluids B **5** (1993) 3217.
[19]. KOLESNICHENKO, Ya. I., Nucl. Fusion **20** (1980) 727.
[20]. SHINOHARA, K. et al., Nuclear Fusion **41** (2001) 603.
[21]. GRYAZNEVICH, M.P. and SHARAPOV, S.E. Plasma Phys. Control. Fusion **46**, S15 (2004)
[22]. BERK, H. L. et al., Phys. Plasmas **6** (1999) 3102.
[23]. BREIZMAN, B. N. et al., Phys. Plasmas **4** (1997) 1559.
[24]. PINCHES, S. D. et al., 1998 Comput. Phys. Commun. **111** (1998) 131.
[25]. PINCHES, S. D. et al., Plasma Phys. and Contr. Fusion **46** (2004) S47.
[26]. TESTA, D. et. al., Nucl. Fusion 43, 479 (2003).
[27]. FU, G.Y. et. al, Phys. Plasmas 11, 4036 (1996).
[28]. JAUN, A. et. al, Phys. Plasmas 5, 2952 (1998).

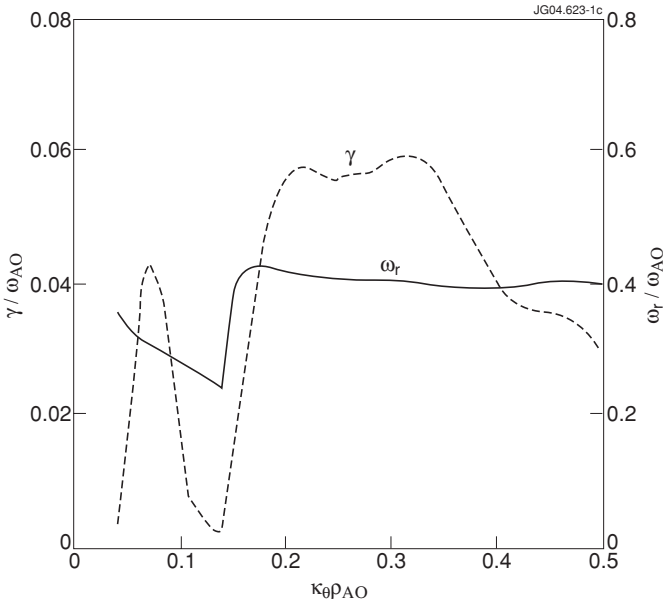

Figure 1: Real frequencies (solid line) and growth rates (dashed line) versus $k_\theta\ \rho_{A0}$ for $s = 0.5$, $\alpha = 2.0$, $\bar{\varepsilon}q = 2.0$, $\beta_{E0} = .06$, $V_{E0} / V_{A0} = 0.7$, $L_{P0} / R = -0.1$, $\eta = 1.0$, $\eta_E = 1.0$, $\theta_b \in [80^0, 120^0]$

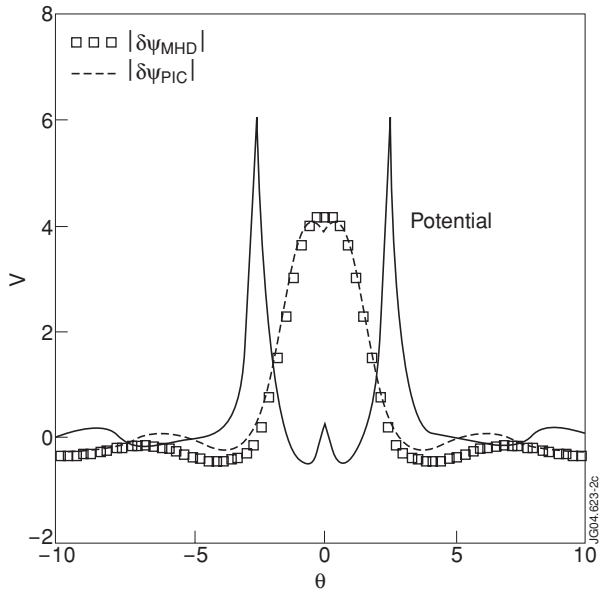

Figure 2: Potential V (solid line) and mode structures of the αTAE (squares) and its kinetic excitation (dashed line) versus θ for the case of $k_\theta\ \rho_{A0} = 0.32$ in Fig. 1.

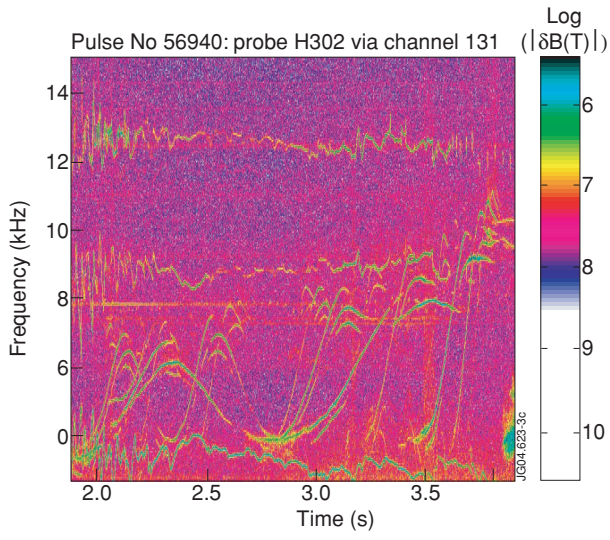

Figure 3: Spectral lines observed on JET show bending at lowfrequency around 43.8s for several n-modes.

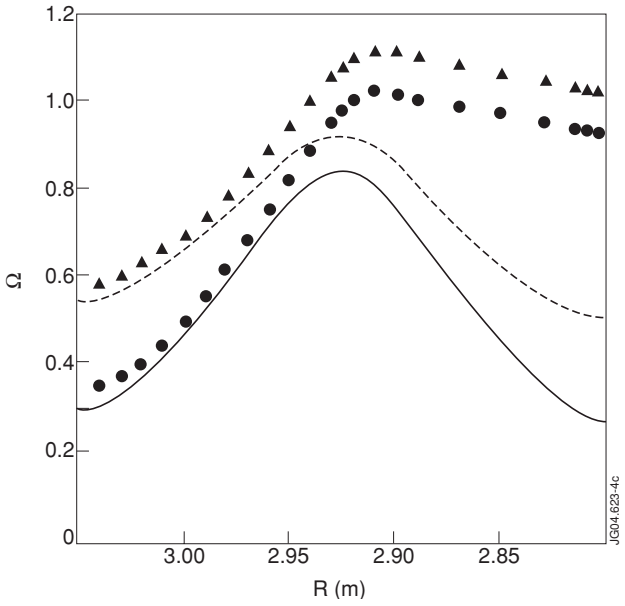

Figure 4: Effect of plasma pressure on mode frequency for n = 3 and m= (12, 11) as a function of the safety factor q_0. Solid curves represent the MHD continuum and the triangular and circular points are for beta values of 0.005 and 0.0015 respectively.

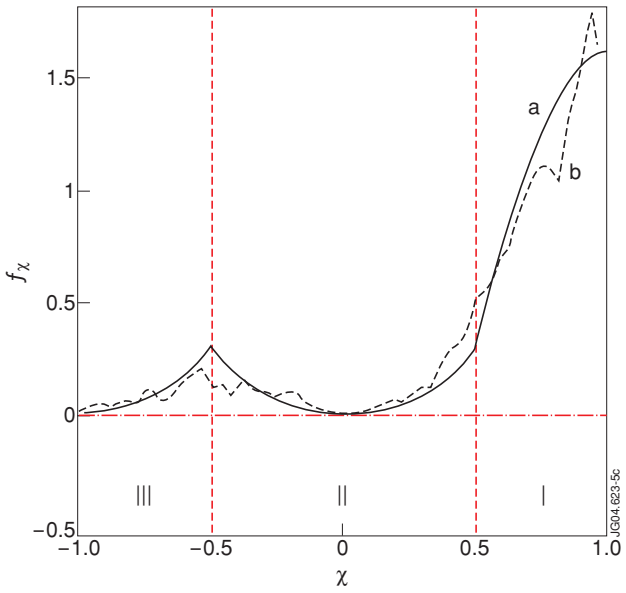

Figure 5: Ion pitch angle distribution, f c ,as function of the pitch angle χ.The different pitch angle region correspond to: (i) co-passing beam ions; (iii) trapped ions: (iii) counterpassing ions. Curve (a) is the distribution predicted from the analytic model, while curve (b) is the distribution function that is generated by the TRANSP Monte-Carlo algorithm.

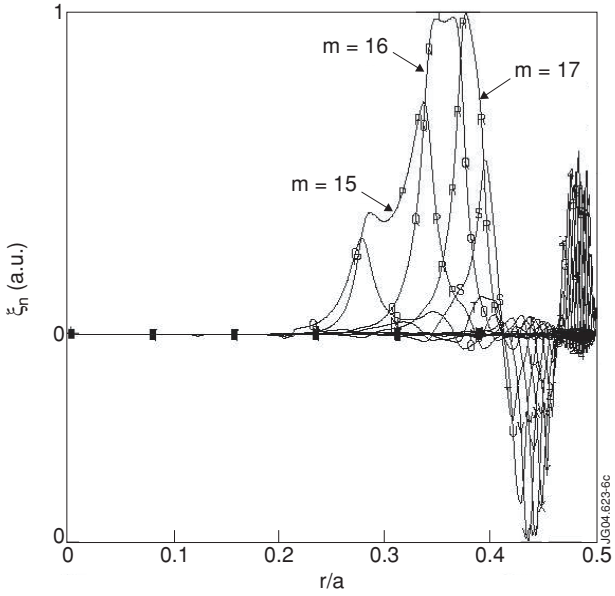

Figure 6: Global TAE eigenmode. Note eigenmode is not excited in the central region.

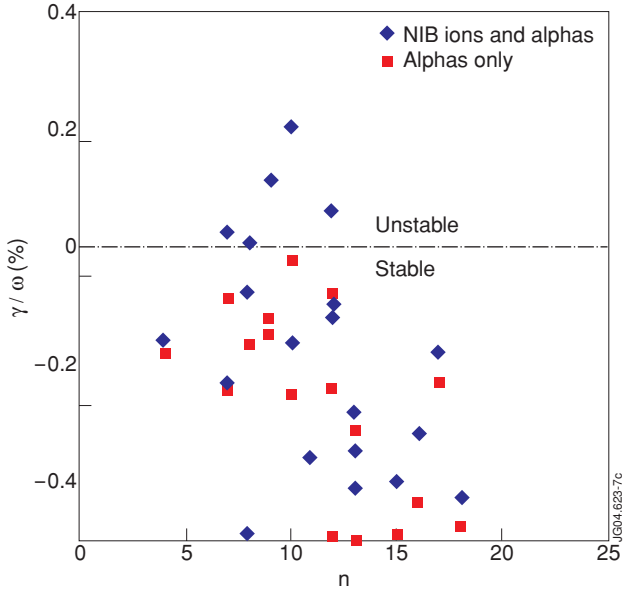

Figure 7: Toroidal mode number dependence of the TAE growth rates for the cases with the drive from alpha particles alone (squares) and from both the NBI ions and alpha particles (diamonds).

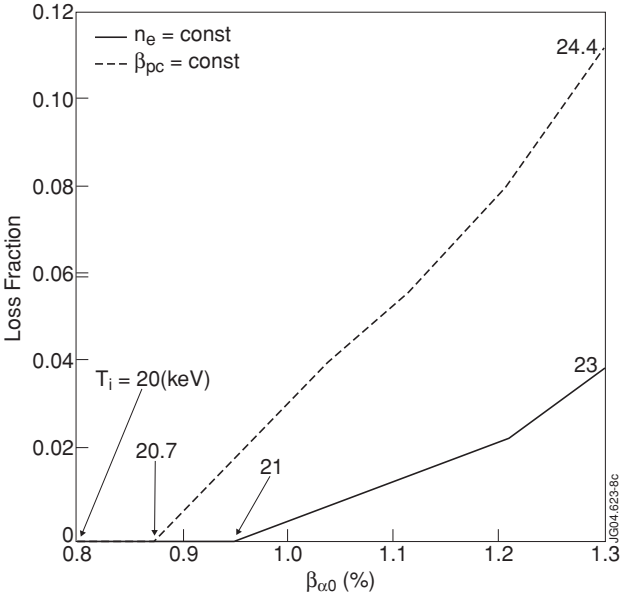

Fig. 8: Fraction of alpha particle loss as a function of the alpha particle beta value as the core ion temperature varies from 20kev to 24.4 kev with the plasma densityconstant (solid curve) or the plasma beta constant (dotted curve).

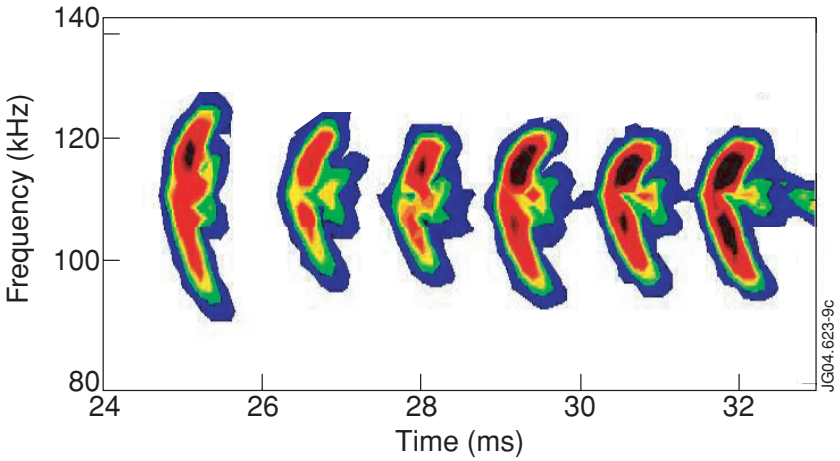

Figure 9. Frequency sweeping observed in MAST experiment, Pulse No 5568

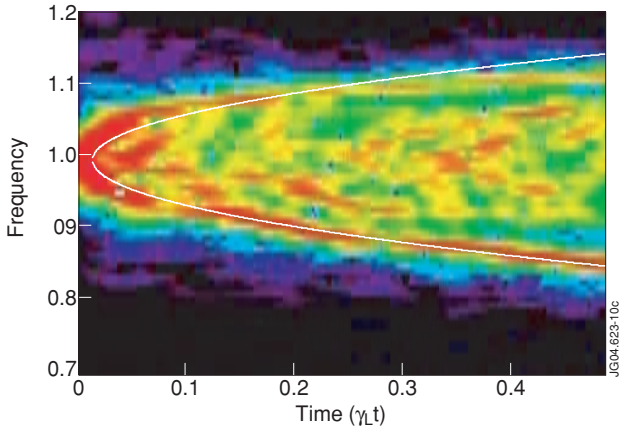

Figure 10: Frequency simulation of the MAST from the HAGIS code showing up-down frequency splitting from phase space structure formation.

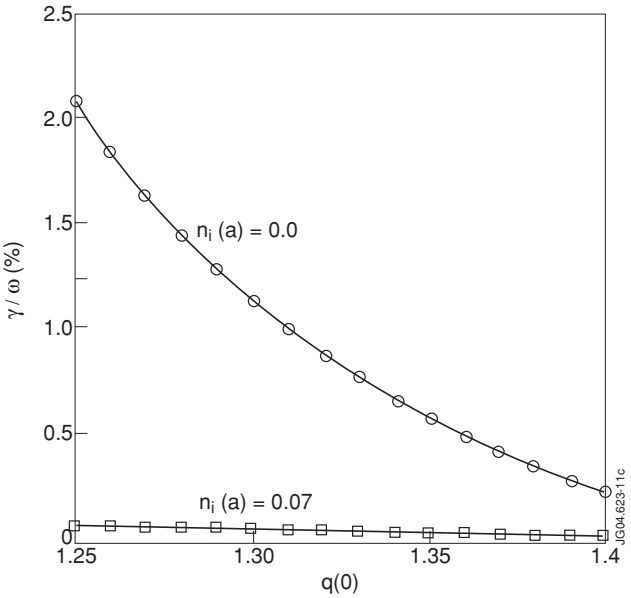

Figure 11: Relative continuum damping rate, γ / ω, versus q(0).